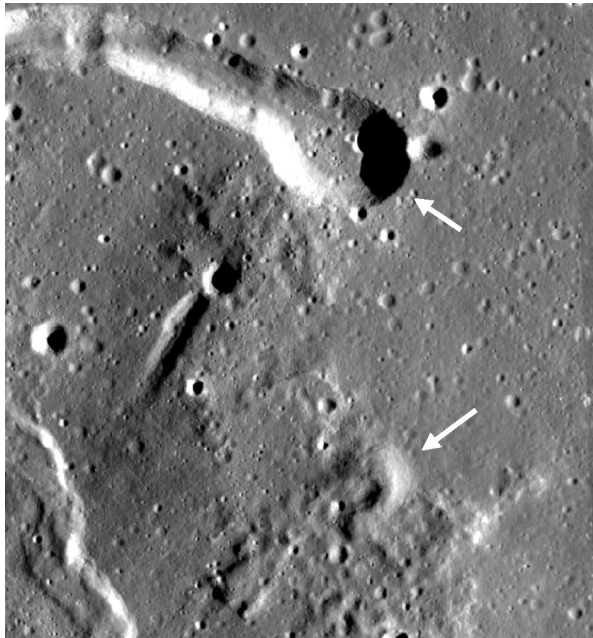


**ERUPTION CONDITIONS DEDUCED FROM THE EXTENTS OF PYROCLASTIC CONSTRUCTIONAL FEATURES SURROUNDING VOLCANIC VENTS ON THE MOON.** L. Wilson<sup>1,2</sup> and J. W. Head<sup>2</sup>, <sup>1</sup>Lancaster Environment Centre, Lancaster University, Lancaster LA1 4YQ, U.K., l.wilson@lancaster.ac.uk <sup>2</sup>Department of Earth, Environmental, and Planetary Sciences, Brown University, Providence RI U.S.A., james\_head@brown.edu

**Introduction:** We show how volcanic constructs in the form of pyroclastic cones surrounding vents, and raised rims at the edges of sinuous rille source depressions, can provide data on magma volatile contents and magma volume eruption rates (Fig. 1).



**Figure 1:** Examples of breached pyroclastic cone (lower arrow) and sinuous rille source vent (upper arrow) in the Marius Hills volcanic complex. Image is 11 km wide and centered on 13.58 N, 56 W.

**Theory:** Lunar fire-fountains had much in common, as regards their dynamics, with the umbrella-shaped volcanic "plumes" on Io, though the lunar examples were very much smaller because lunar magmas contained only a few 100 to ~3000 ppm of volatiles [1- 5], 100 to 1000 times less than the amounts of recycled sulfur compounds driving Io's largest explosive eruptions [6]. The Apollo samples show [7-10] that lunar magmas were commonly disrupted into pyroclasts with diameters in the range 100 to 1000 microns due to the extreme expansion into the lunar vacuum of the bubbles of exsolved gas. Allowing for sorting effects as different sized pyroclasts decouple from the expanding gas at different gas pressures and a plausible compositional mixture for lunar volatiles [3-5, 11, 12], the maximum range of pyroclasts  $R$  is given by [13] as

$$R = 5.734 n \quad (1),$$

where  $R$  is measured in meters and  $n$  is the total released gas mass fraction measured in ppm.

Accumulation of pyroclasts around vents can produce cinder- and spatter-cones depending on the opacity of the fire fountain, and the radius of the cone can give the magma volatile content via eq. (1). In a lunar fire-fountain containing a high concentration of small pyroclasts, significant heat can only be lost from within an outer shell extending inward from the edge of the fountain by a critical distance  $X$ , which may be termed the opacity depth. For a point-source vent forming a circularly-symmetric fountain,

$$X = (6.17 d g^{1/2} R^{5/2}) / F \quad (2),$$

where  $F$  is the total erupted dense-rock-equivalent magma volume flux. We see shortly that it is convenient to have  $X$  as a fraction of the maximum pyroclast range  $R$ , i.e.,

$$X / R = (6.17 d g^{1/2} R^{3/2}) / F \quad (3).$$

**Analysis:** Using these relationships we explore likely eruption conditions for two classes of lunar volcanic features, breached cinder- and spatter-cones, and sinuous rille source depressions.

*1. Pyroclastic cones.* Wan et al. [14] measured the morphologies of 360 cones in the Marius Hills complex, assigning them to morphological groups. Their group most readily identifiable as being formed by the accumulation of pyroclasts is the "C-shaped" cone group, where the morphology clearly suggests escape of a lava flow by the breaching of a cinder- or spatter-cone wall. 75% of these cones have radii  $R$  between 400 and 700 m. Converting cone radii to implied magma volatile contents, 72% of the 32 C-shaped cones have  $n$  in the range 70-110 ppm. The radius of the central depression in these cones, marking the location of the hot part of the lava pond that they contained, was typically 20% of the radius of the cone, implying that the opacity depth,  $X$ , was typically a maximum of 80% of the maximum radius,  $R$ , to which pyroclasts were ejected. Table 1 shows values of the quantity  $X/R$  found from eq. (3) for the above range of magma volatile contents  $n$  and the corresponding maximum ranges  $R$  for each of a series of possible magma volume eruption rates. The combinations of values of  $R$  and  $F$  that produce the observed value of  $X/R$ , 80%, are highlighted. The implication is that the

breached cones were produced by eruptions having magma discharge rates between  $\sim 25$  and  $60 \text{ m}^3 \text{ s}^{-1}$ .

**Table 1:** Values of  $X/R$  for a range of values of magma volume eruption rate  $F$  in  $\text{m}^3 \text{ s}^{-1}$  for measured maximum clast ranges  $R$  in meters and implied magma volatile contents  $n$  in ppm for breached cones.

$n$	$R$	$F = 25 \quad 30 \quad 40 \quad 50 \quad 60$				
		Values of $X/R$ as a percentage				
60	344	60	50	38	30	25
72	413	<b>80</b>	66	49	40	33
82	470	96	<b>80</b>	60	48	40
99	568	100	100	<b>80</b>	64	53
115	659	100	100	100	<b>80</b>	66
130	745	100	100	100	96	<b>80</b>
144	826	100	100	100	100	93

2. *Sinuuous rille source depressions.* Using the lunar sinuous rille catalog of [15], [16] found the radii of the depressions defining the locations of the hot lava ponds that fed the lava flows thermally eroding the rilles. 86% of the ponds have radii between 400 and 4800 m, implying magma volatile contents between 70 and 840 ppm. The ponds all display a low ring of accumulated pyroclasts surrounding the pond depression. In all cases, the heights of these rings are a small fraction of the depth of the depression, but their presence indicates that the fire fountain operating during the eruption was not opaque all the way to its outer edge. Measurements on a sample of the depressions imply that the opacity depth,  $X$ , was typically a maximum of 40% of the maximum radius,  $R$ , to which pyroclasts were ejected. Table 2 shows the values from eq. (3) for the narrower pyroclastic rings surrounding the sinuous rille sources. The 40% value of  $X/R$  implies magma discharge rates between  $\sim 50$  and  $2000 \text{ m}^3 \text{ s}^{-1}$ .

**Table 2:** Values of  $X/R$  for a range of values of magma volume eruption rate  $F$  in  $\text{m}^3 \text{ s}^{-1}$  for measured maximum clast ranges  $R$  in meters and implied magma volatile contents  $n$  in ppm for sinuous rille source ponds.

$n$	$R$	$F = 50 \quad 100 \quad 500 \quad 900 \quad 1300 \quad 1700$					
		Values of $X/R$ as a percentage					
60	344	30	15	3	2	1	1
72	413	<b>40</b>	20	4	2	2	1
116	665	81	<b>40</b>	8	4	3	2
335	1921	100	100	<b>40</b>	22	15	12
500	2867	100	100	72	<b>40</b>	28	21
635	3641	100	100	100	58	<b>40</b>	30
760	4358	100	100	100	75	52	<b>40</b>
900	5161	100	100	100	97	67	51

**Discussion:** The magma volatile contents found here for both types of feature lie within the range estimated by other methods [1-5]. The magma discharge rates for the breached cones are similar to those for mild fire-fountaining activity on Earth [17]. The magma discharge rates found for the sinuous rille source vents are smaller than those estimated from the depths of the rilles,  $\sim 10^4 \text{ m}^3 \text{ s}^{-1}$  [18-20] by about a factor of 10. The most likely explanation is that the magma discharge rates declined towards the ends of the eruptions and the low pyroclast rims surrounding the source depressions record this waning stage. This interpretation is supported by the fact that the volumes of the rim deposits are extremely small fractions of the volumes of erupted lava needed to thermally erode the rille channels.

The results given here have been obtained using the average value, for each of the two types of feature, of the ratio  $X/R$ . A more detailed analysis is underway using the measured values of  $X$  and  $R$  for each individual feature.

**References:** [1] Milliken R. E. and Li S. (2017) *Nature Geosci.*, 10, 561–565. [2] Li S. and Milliken R. E. (2017) *Science Advances* 3, 1–11. [3] Rutherford M. J. et al. (2017) *Amer. Mineral.*, 102, 2045-2053. [4] Renggli C. J. et al. (2017) *GCA*, 206, 296–311. [5] Newcombe M. E. et al. (2017) *GCA*, 200, 330–352. [6] Leone G. et al. (2011) *Icarus*, 211, 623-635. [7] Heiken G. H. et al. (1974) *GCA*, 38, 1703-1718. [8] McKay D. S. et al. (1978) *Proc. LPSC 9th*, 1913-1932. [9] Arndt J. et al. (1984) *JGR*, 89, C225-C232. [10] Delano J. W. (1986) *JGR*, 91, 201-213. [11] Saal A. E. et al. (2008) *Nature*, 454, 192-195. [12] Hauri E. H. et al. (2011) *Science*, 333, 213-215. [13] Morgan C. et al. (2021) *JVGR*, 413, 107217. [14] Wan S. et al. (2022) *JGR-Planets*, 127, e2022JE007207 [15] Hurwitz D. M. et al. (2013) *PSS*, 79-80, 1-38. [16] Wilson L. & Head J. W. (2021) *LPS*, LII, abs. #1226. [17] Parfitt E. A. and Wilson L. (2008) *Fundamentals of Physical Volcanology*, Blackwell. [18] Wilson L. and Head J. W. (1980) *LPS*, XI, 1260-1262. [19] Head J. W. and Wilson L. (1980) *LP.*, XI, 426-428. [20] Head J. W. and Wilson L. (1981) *LPS*, XII, 427-429.